Linking surface-fire behavior, stem heating, and tissue necrosis

A.S. Bova and M.B. Dickinson

Abstract: Data from 69 experimental, small-plot fires are used to describe relationships among fire intensity, bark-surface heat flux, and depth of necrosis in stem tissue for red maple (*Acer rubrum* L.) and chestnut oak (*Quercus prinus* L.). A tetrazolium staining technique was used to determine the depth of necrosis in tree boles subjected to fires with intensities of 20 to 2000 kW/m. Over a range of bark moistures (28%–83%) and bole diameters (3–20 cm), depth of necrosis appears to be primarily a function of fire intensity, flame residence time at the stem, and the corresponding time-integrated heat flux at the bark surface. Our results, along with known relations between bole diameter and bark thickness, and improved models of fire behavior and heat transfer, may be useful for estimating tree mortality resulting from prescribed fires.

Résumé : Les données provenant de 69 petites parcelles brûlées à des fins expérimentales sont utilisées pour décrire les relations entre l'intensité du feu, le flux de chaleur à la surface de l'écorce et la profondeur de la nécrose dans les tissus du tronc de l'érable rouge (*Acer rubrum* L.) et du chêne des montagnes (*Quercus prinus* L.). Une technique de coloration au tétrazolium a été utilisée pour déterminer la profondeur de la nécrose dans le tronc des arbres exposés à des feux dont l'intensité variait de 20 à 2000 kW/m. Pour une gamme de teneurs en humidité (28 % – 83 %) et de diamètres du tronc (3–20 cm), la profondeur de la nécrose semble principalement fonction de l'intensité du feu, du temps de résidence des flammes sur le tronc et du flux de chaleur pour la durée correspondante à la surface de l'écorce. Les résultats combinés aux relations connues entre le diamètre du tronc et l'épaisseur de l'écorce, ainsi que de meilleurs modèles du comportement du feu et des transferts de chaleur, peuvent être utiles pour estimer la mortalité des arbres à la suite de brûlages dirigés.

[Traduit par la Rédaction]

Introduction

Flames in surface fires transfer heat into tree stems, which results in elevated temperatures that can cause tissue necrosis to various depths. Stem death can result when tissue necrosis occurs through the live bark to the depth of the vascular cambium and around the tree's circumference. The literature is extensive on surface fires (Fons 1946; Anderson and Rothermel 1965; Nelson and Adkins 1986), stem heating (Rego and Rigolot 1990; Costa et al. 1991; Pinard and Huffman 1997; Potter and Andresen 2002), and plant-tissue necrosis (Lorenz 1939; Hare 1961; Kayll 1963; Levitt 1980; Dickinson et al. 2004; Dickinson and Johnson 2003). Proposed physical models couple the component processes in a variety of ways (Martin et al.1969; Peterson and Ryan 1986; Mercer et al. 1994; Gutsell and Johnson 1996; Jones 2003; Dickinson and Johnson 2004), but there are no combined data on fire behavior, stem heating, and tissue necrosis.

In this paper, we link fire behavior to stem heating, which is in turn linked to the radial depth of tissue necrosis in chestnut oak (*Quercus prinus* L.) and red maple (*Acer rubrum* L.), two common species in the central hardwood forests of the eastern United States. Experimental burns were conducted during the dormant season to best simulate the prevailing and historical fire season (Sutherland et al. 2003). Both species have virtually identical responses to stem heating, but, at a given diameter, chestnut oak has greater bark thickness than red maple and, therefore, greater protection from damage. Combined with a better understanding of heat transfer from flames to stems, our equations may be used to predict stem death (and tree death for stems that do not resprout).

Received 23 April 2004. Accepted 14 December 2004. Published on the NRC Research Press Web site at http://cjfr.nrc.ca on 22 April 2005.

A.S. Bova[1] **and M.B. Dickinson.** USDA Forest Service, Northeastern Research Station, Forestry Sciences Laboratory, 359 Main Road, Delaware, OH 43015-8640, USA.

[1]Corresponding author (e-mail: abova@fs.fed.us).

Heat flux at the stem surface

Models of heat and moisture transfer in cylindrical objects, such as tree boles, assume a known temperature or heat-flux regime at the surface (e.g., Costa et al. 1991; Mardini et al. 1996). It is difficult to model tree bole surface heat flux because of the variability in flame height, depth, residence time, changes in intensity due to varying winds and the changing distance of the flame from the tree. We developed equations based on physical relationships between fire behavior and surface heat flux, and between surface heat flux and tissue necrosis, charting a course between mechanism-free statistical models and, as yet, poorly validated process models.

Flames emit energy in the form of thermal radiation, the total power of which depends upon the flame's length, width, and average thickness. As a surface fire approaches a bole, the incident thermal radiation increases until the flame contacts it, at which time convective heating usually becomes

 doi: 10.1139/X05-004

the dominant mode of heat transfer. Before contact, the heat flux at the bole resulting from radiation is a function of the flame's geometry and distance, as well as the diameter of the bole. The net heat flux at the surface of a bole when surrounded by flames is

$$[1] \quad q'' = (h_{con} + h_{rad})(T_{surface} - T_{flame}) + q''_{evaporation}$$

where q'' has units of kW/m^2. The coefficient of convection, h_{con} (kW·m^{-2}·K^{-1}), is a function of the velocity of flame gases and bark surface characteristics. The coefficient of radiation, h_{rad} (kW·m^{-2}·K^{-1}), is highly dependent on the surface and flame temperatures, $T_{surface}$ and T_{flame} (K), and the ratio of the thermal radiation emitted by the flame to that of a blackbody at the same temperature. This ratio, called emissivity, is determined by the average thickness of the flame and its soot content. By convention, the sign of q'' is negative if the net heat transfer is to the surface ($T_{surface} < T_{flame}$) and positive otherwise.

In the literature on wildland fires, the rate of heat release per unit length of fireline is called the fire intensity (or Byram index), I (kW/m) (Johnson 1992), and is defined as

$$[2] \quad I \equiv HWS$$

where H is the average heat of combustion of the surface fuel(s) (kJ/kg), W is the fuel consumption (kg/m^2), and S is the rate of spread of the flame (m/s). The average low heat of combustion for a variety of forest fuels is 18 700 kJ/kg (Johnson 1992). In fire intensity calculations, the low heat value is decreased by 15%–20% to account for radiative loss (Nelson and Adkins 1986). The resulting value, 15 000 kJ/kg, was used in our calculations of fire intensity. Fuel consumption, W, should be only that portion of the fuel consumed during flaming combustion, but this is a fraction difficult to estimate in practice. Consequently, Johnson (1992) and Nelson and Adkins (1986) suggested using total fuel consumption in estimates of fire intensity.

Fire intensity determines the base-to-tip length of surface flames (length, where length $\propto I^{2/3}$, Yuan and Cox 1996) and, therefore, their radiative area and total radiative power. As radiative power increases, the distance at which flames significantly heat the bole also increases, implying greater preheating of the bole before the flame arrives. Intensity also governs the average upward velocity of surface flames (velocity, where velocity $\propto I^{1/3}$, Nelson 1988), which is a major factor in the convective heating of the bole when the flame makes contact. A given fire intensity can occur over a large range of fuel consumption (Johnson 1992), so intensity does not, by itself, indicate the total heat energy released per unit area (HW) near a bole. However, fire intensity can be multiplied by a characteristic time value, such as the flame residence time, to give a measure of total heat energy that is released per unit length of fireline (kJ/m). The net heat flux at the surface of the bole, or a significant portion of it, should, therefore, be a function of, among other variables, intensity and the flame residence time at the surface of the stem:

$$[3] \quad Q'' = \int q''\mathrm{d}t \approx f(I, \tau, \ldots)$$

where Q'' has units of kJ/m^2 and τ (s) is the time over which flames are present at a given location on the surface of the bole. Note that the time of radiative heating before flame contact could be added to τ to produce a total "time of effect," but in practice this would be more difficult than estimating flame residence times.

Stem heating

Given known boundary conditions for surface temperature or heat flux, the heat equation can be used to calculate the temperature profile within a cylindrical structure such as a bole (Incropera and DeWitt 2002). However, because of the varying surface heat flux, moisture outflux, and internal conditions, a numerical model usually is required to estimate internal temperatures that vary with depth and over time (Jones et al. 2004). As an alternative, we propose equations based on the following physical principles.

Over the time of heating and cooling, t (s), the thermal front will diffuse toward the centre of the bole to a depth, $\delta \propto (\alpha t)^{1/2}$ (mm), where α (m^2/s) is the thermal diffusivity of bark and wood (assumed here to be roughly equal). Further, assuming that the heat flux around the bole is uniform, the average excess energy density, U (kJ/m^3), of the heated portion of the bole will reach a maximum (as will the surface temperature) just before cooling begins and can be approximated as

$$[4] \quad U = Q''\left(\frac{2R}{2R\delta - \delta^2}\right)$$

where R is the bole radius (m) and the term in parentheses is the ratio of the surface area of the bole to the volume of the heated cylinder of circumference $2\pi R$ and thickness δ.

The term for heat loss by evaporation is present in eq. 1, because heat transfer into the stem has been shown to be driven largely by conduction and heat sinks associated with bark moisture (Rego and Rigolot 1990). Diffusion or migration of moisture depends on the pressure, temperature, and moisture gradients within the stem during the heating process. Using conservation of mass and energy in addition to experimental correlations, Mardini et al. (1996) successfully modeled mass change resulting from pyrolysis of wooden dowels, but the model did not correctly predict moisture loss in dowels exposed to the rapid heating characteristic of stems in surface fires. For simplicity, outward heat flux due to moisture loss is not explicitly included in the model below, and we have assumed that the moisture outflux is proportional to the heat influx.

Tissue necrosis

Tissue necrosis can be described by a temperature-dependent rate process:

$$[5] \quad \frac{\mathrm{d}V}{\mathrm{d}t} = -kV$$

where V is some indicator of viability, such as cell survival or tissue respiration, and k (s^{-1}) is the rate of decline in viability (Johnson et al. 1974). The rate parameter, k, at a given depth is a function of temperature and can be adequately described by the Arrhenius equation:

$$[6] \quad k(t) = Z\exp\left(-\frac{E}{\Re T(t)}\right)$$

where $T(t)$ (K) is temperature at time t; Z is a pre-exponential factor (s^{-1}), E is the activation energy ($J \cdot mol^{-1}$), and $\Re$ is the universal gas constant (8.31 $J \cdot mol^{-1} \cdot K^{-1}$). The exponent is simply a time-dependent ratio of energy densities. Viability declines as tissues are heated above approximately 40 °C, and final viability at a given depth after a stem has cooled is described by

$$[7] \qquad V = A \exp\left(-\int_t k(t)\,dt\right)$$

where A is a constant. Note that at a given depth, the final viability depends on the time spent over 40 °C and that the time required to kill tissue decreases as the temperature rises above this lower limit. In other words, the final viability at a given depth depends on the area under the temperature–time curve (Martin et al. 1969; Mercer et al. 1994; Mercer and Weber 2001). As the thermal front moves toward the centre of the bole, the average rate of decline in viability decreases along with the average energy density (i.e., average excess temperature).

We hypothesize that at some depth below the bark surface, r (mm), the rate of decline in viability integrated over the time above 40 °C (or the average rate multiplied by this time) will be just sufficient to lower the viability to an (arbitrary) value at which an irreversible wounding response, involving the production of secondary compounds followed by programmed cell death, begins (Dickinson and Johnson 2004). Thus, tissue necrosis propagates through the bole as a threshold that is a function of time and temperature. The necrosis threshold should be identifiable experimentally.

We assume, and numerical analysis shows, that the depth below the bark surface at which a given value of the rate of reaction integral (exponent of eq. 7) occurs is a roughly linear and increasing function of the average energy density, U. Further, we assume that the minimum value of this integral that corresponds to necrosis does not vary greatly between trees or species. If these assumptions are correct, the maximum energy density averaged over the depth of necrosis should be roughly constant, that is, the volume (or depth) of necrosis should be proportional to the integrated heat flux, giving

$$[8] \qquad 2Rr - r^2 \approx CQ''R$$

where the depth of necrosis, r, is substituted for the δ in eq. 4, and C is a constant. Note that when $r << R$, the relationship may be approximated by

$$[9] \qquad r \approx CQ''$$

In other words, the depth of necrosis depends simply on the time-integrated heat flux, and, by eq. 3, is ultimately a function of fire intensity, flame residence time at the stem, and other factors not explicit here (e.g., air temperature).

Methods

In spring and fall 2002 and in spring 2003, a series of 42 plot burns and 7 rope burns were conducted in the Vinton Furnace Experimental Forest (VFEF) in southern Ohio. Plot burns were conducted using rectangular plots that ranged from 3 m × 7 m to 4 m × 8 m (Fig. 1). The fuel bed consisted of leaf litter, straw, poplar excelsior, corn stalks, milled softwood sticks (0.95 cm × 0.95 cm cross section, 60 cm long) or a combination of these.[2] The plots were constructed so that a target tree was positioned along the plot centreline and far enough along the bed so that there was sufficient time for the approaching fire to reach a relatively uniform rate of spread. Fires were started by drip torch at one end of the plot and allowed to burn well past the target tree. Flame heights, rates of spread, and weather variables were recorded. Five of the burns departed from the standard configuration in that wood cribs were built against the target tree from six alternate layers of the softwood sticks described above; instrumentation remained the same.

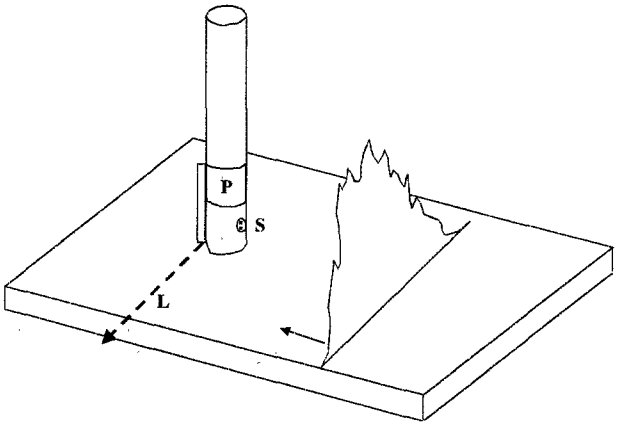

Fig. 1. Schematic of plot burns. A line fire moves toward a tree bole fitted with a heat-flux sensor (S). The patch (P) on the bole represents cable shielding that also covers the cables and leads on the rear of the tree. Leads (L) were buried in a shallow trench leading to a data logger outside the plot, or, in some cases, immediately behind the target bole.

The target tree was instrumented with a Medtherm™ heat-flux sensor (Huntsville, Alabama, USA) inserted through the bole, 15 cm above the soil surface; the sensor face was positioned flush with the bark surface on the side of the approaching flames (Fig. 1). These sensors are of the Schmidt–Boelter (thermopile) type and provide readings of total (convective plus radiant) and radiant heat flux. Data were collected at 1-s intervals with a Campbell CR10X data logger (Logan, Utah, USA). Values of the total heat flux over time, Q'', were calculated by summing values of total heat flux that exceeded 2 kW/m^2 (i.e., heat flux clearly above initial background flux). Flame residence time at the bole was estimated from plots of convective (total minus radiative) heat flux versus time (flame presence is indicated by a sudden rise and plateau in such plots).

Rope burns (Uhl and Kauffman 1990) consisted of a single- or double-circumference length of rope that was soaked in fuel oil and coiled around the target tree 8 cm below the heat-flux sensor. The rope was attached with nails and the

[2] Supplementary data for this article are available on the Web site or may be purchased from the Depository of Unpublished Data, Document Delivery, CISTI, National Research Council Canada, Ottawa, ON K1A 0S2, Canada. DUD 3644. For more information on obtaining material refer to http://cisti-icist.nrc-cnrc.gc.ca/irm/unpub_e.shtml.

tree was instrumented using the same method as for the plot burns. After ignition, the rope was allowed to burn for several minutes, in contrast with the relatively short flame residence times (10–30 s) in the plot burns.

Ceramic wool covered with fire-shelter material was used to shield exposed cables, leads, and equipment. The shielding was wrapped around the target boles 20 cm above the heat-flux sensors, to protect the bases and leads of small thermocouple probes, and around the heat-flux sensor wires protruding from the back of the boles (Fig. 1). Leads were connected to a shielded data logger placed behind the tree, or, more commonly, were buried and directed to a logger placed off the plot (Fig. 1).

To increase the number of trials during fall 2002 and spring 2003, freshly cut, 1.5 m long boles were erected in a reusable plot and secured with a section of rebar and guywires. Plot size and instrumentation did not change. The time between cutting, exposure to flame, and staining for the measurement of the depth of necrosis was a few hours. Cut boles did not appear to respond differently from uncut boles (see Results).

Fuels were weighed before being spread over the plots in order to estimate fuel loading. Fuels were consumed completely; therefore, loading was taken as equivalent to fuel consumption and no adjustment was made for ash content. These data, along with measurements of the rate of spread and an assumed heat of combustion (15 000 kJ/kg), were used to calculate Byram intensities according to eq. 2. Using total fuel consumption, not the portion consumed during only flaming combustion, could lead to an overestimate of fire intensity in burns with significant glowing combustion (e.g., those with thicker fuel components, such as corn stalks). However, as in Nelson and Adkins (1986) and Johnson (1992), we used total fuel consumption in our estimates of fire intensity.

The depth of necrosis in stems was measured radially from the bark surface and was determined by staining with tetrazolium trichloride (TTC) to detect respiration activity (e.g., Parker 1953; Towill 1975; Caldwell 1993). TTC is reduced to a pink formazan in live tissues but remains colorless in dead tissue (Kayll 1963). A basal section was cut from each experimental tree with a chainsaw and transported to the VFEF workshop, where thin (2–4 mm) cross sections were removed at 10 and 20 cm above ground with an electric circular saw. Sections were vacuum infiltrated with a 0.8% (*m*/*v*) TTC solution made in 0.05 mol/L potassium phosphate buffer (pH 7.5) and stored in the dark for 18–24 h at room temperature. Depth of necrosis, bark thickness, and actual depth of the thermocouple probe tips were measured to the nearest 0.1 mm with callipers. Depths of necrosis and bark thickness were averaged over a total of 10 measurements taken at heights of 10 and 20 cm along the bole (5 cm below and 5 cm above the heat-flux sensor). Five measurements were taken at each height: one at the vertical centreline through the heat-flux sensor centre, two at distances of 1 and 2 cm to the left of the centreline, and two at distances of 1 and 2 cm to the right of the centreline. A two-sample paired *t*-test showed that the average depths of necrosis were not significantly different between 10 and 20 cm (mean diff. = 0.2 mm, $p = 0.35$, df = 29).

Equations 10 and 11 were generated from simple linear regressions of untransformed data. To homogenize the variance, the variables in eqs. 12 and 13 were natural-log transformed before a multivariable linear regression was performed. All statistical analyses were performed using SYSTAT® version 9 software (Systat Software, Inc., Point Richmond, California, USA). The number of replicate trees in the figures and regressions below may vary depending on available data. For instance, there were more burns in which heat flux and depth of necrosis were measured than in which fire intensity and necrosis were measured.

Fig. 2. Red maple (*Acer rubrum* L., 10 cm diam.) section stained with tetrazolium. The abrupt color change indicates the transition from dead to live sapwood.

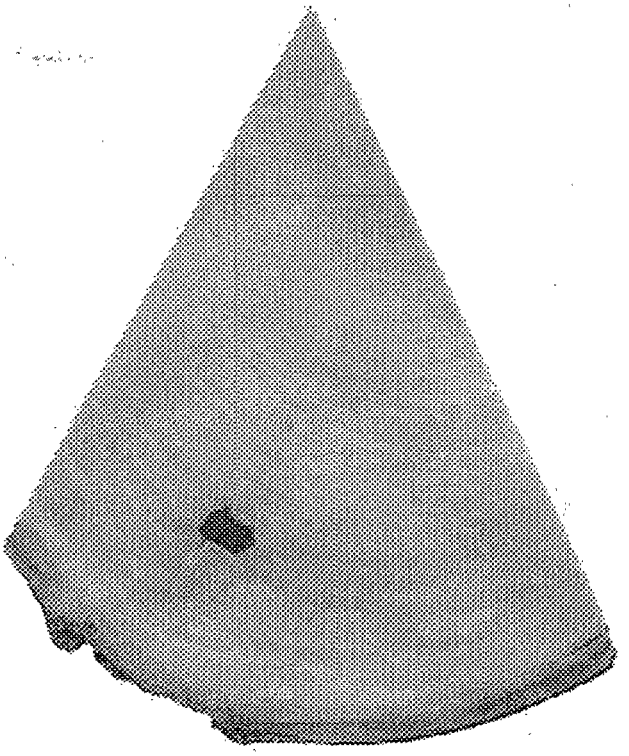

Results

Tissue kill appeared to propagate as a wave into stems, and there was typically a sharp transition between live and dead tissue (Fig. 2). Attempts to discriminate between live and dead conifer tissues stained with TTC were not successful because of discoloration associated with their wounding response.

Equations 8 and 9 imply a direct relation between surface heat flux and the depth of necrosis below the bark surface. Figure 3 shows the relationship between the depth of necrosis and the time-integrated heat flux, Q''. The circled point is a statistical outlier (studentized residual = –4.75) and seems to be the result of a decalibrated heat-flux sensor. The statistical outlier is not included in the regression. The constant of the linear, least-squares regression equation was not significantly different from zero at the 5% confidence level, so the relation is cast in the zero-intercept form

[10] $$r = 0.002Q''$$

Fig. 3. Average depth of necrosis, r (m), versus the measured heat flux integrated over time, Q'' (kJ/m^2). The trendline does not include the circled outlier.

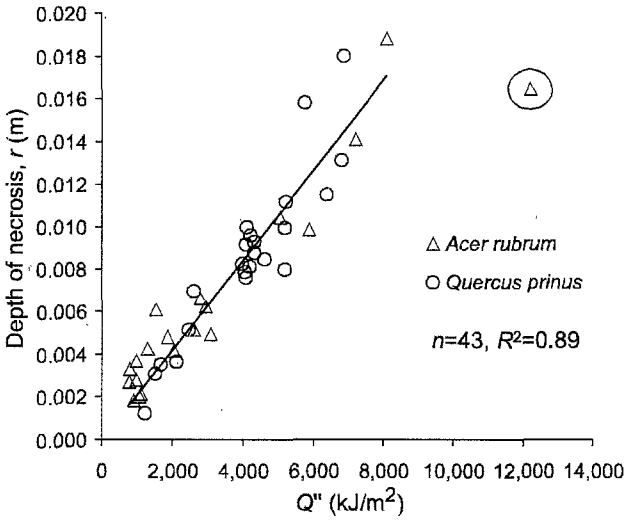

where the depth of necrosis, r, has units of millimetres. The confidence intervals ($p < 0.05$) of the coefficient in eq. 10 overlapped in separate regressions of uncut ($n = 27$) and cut boles ($n = 16$).

Figure 4 shows that the relationship is improved in a regression of the terms in eq. 8. The circled outlier was again omitted. The relation is also linear:

$$[11] \quad 2Rr - r^2 = 0.002Q''R$$

It appears that this form of the necrosis – heat flux relation improved the fit in cases where the depth of necrosis was greater than ~20% of the bole radius.

Equation 3 implies a relation between the fire intensity, time of flame contact, and the time-integrated heat flux. The relation is nonlinear and has the functional form

$$[12] \quad Q'' = 148I^{0.16}\tau^{0.58} \qquad n = 39,\ R^2 = 0.72$$

Based on the linear relation between depth of necrosis and integrated heat flux (eq. 10), we expect that the depth of necrosis will relate to intensity and flame residence time at the surface in a similar form with roughly similar exponents. This is confirmed by a regression (Fig. 5) yielding the equation

$$[13] \quad r = 0.21I^{0.20}\tau^{0.64}$$

Discussion

There is a strong relationship between time-integrated heat flux and depth of necrosis for chestnut oak (*Q. prinus*) and red maple (*A. rubrum*) (Figs. 3 and 4). Integrated heat flux in turn is related to fire intensity and flame residence time at the surface of the bole. The relationships between integrated heat flux and depth of necrosis are similar between species despite differences in bark moisture, density, and thickness. In part, this may be because the thermal diffusivity of bark, and, therefore, the rate of penetration of heat, remains roughly constant among species across a large range of wood densities and moisture contents (Martin 1961). In addition, thermal tolerance appears to be similar between chestnut oak and red maple (Dickinson et al. 2004). A wide range of both broadleaf and conifer species generally differed minimally in thermal tolerance (Dickinson 2002; Dickinson and Johnson 2004). We expected that differences in bark moisture between species would result in differences in kill depth because of differences in heat sinks associated with the drying of their bark, but this effect must have been secondary (see below).

We attempted to relate fire intensity alone to depth of necrosis. As expected, the relationship was significant ($R^2 = 0.27$, $n = 26$) but not satisfactory. Fire intensity is central to flame structure and velocities and, thus, must be used for under-

Fig. 4. Energy density correlation (eq. 11). The area (or volume per unit height) of necrosis (m^2) versus the time-integrated flux, Q'' (kJ/m^2), multiplied by the bole radius, R (m). The trendline does not include the circled outlier.

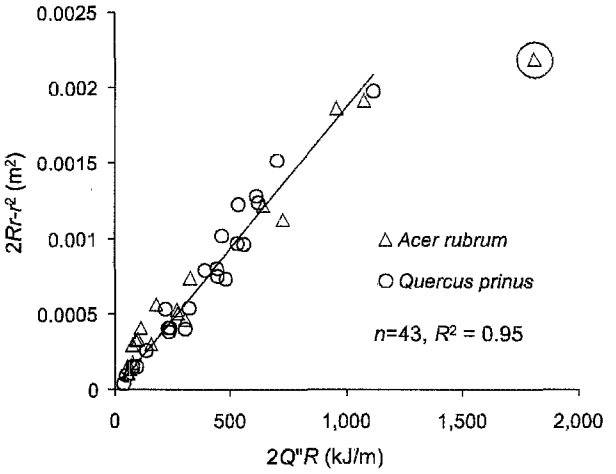

Fig. 5. The natural log of depth of necrosis, r (mm), versus a function of log-transformed fire intensity, I (kW/m), and flame residence time, t (s), at the stem.

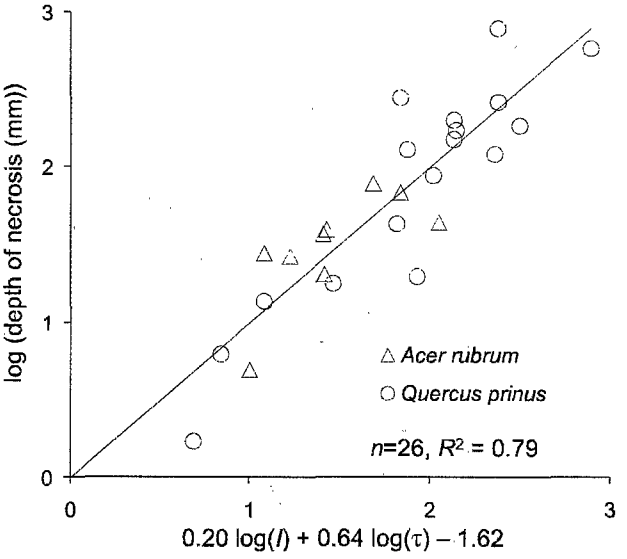

Table 1. Pearson correlation coefficients of flux, DBH, bark moisture, and bark thickness, (n = 34).

	Integrated flux	DBH	Bark moisture	Bark thickness
Integrated flux	1.00	—	—	—
DBH	0.366	1.00	—	—
Bark moisture	–0.441	0.002	1.00	—
Bark thickness	0.640	0.306	–0.387	1.00

standing crown heating (Van Wagner 1973) and crown-fire initiation and spread (Van Wagner 1977). In these experiments, involving a wide range of fuels, flame residence time at the stem predicted integrated flux and necrotic depth (R^2 = 0.68, n = 26) better than fire intensity. However, total heat output in the vicinity of the tree is the best correlate of stem-surface heat flux and is obtained by combining fire intensity with the time during which combustion occurs, here approximated by flame residence time at the tree (eq. 13, Fig. 5).

Stem heating

In these experiments, there were correlations among integrated flux, bark moisture, bark thickness, and tree diameter (Table 1). Diameter and, in particular, bark thickness show a positive correlation with heat flux and are themselves correlated. These correlations were expected, because loading was intentionally increased around larger boles simply to ensure that necrosis was measurable below the thicker bark.

Heat flux through the front portion of the bole appears to have been roughly uniform. Tissue staining indicated that the threshold between viable and necrotic tissue was sharp (Fig. 2) and of relatively uniform depth around all cross sections, which encompassed up to one half of the bole circumference. Note that eq. 12 is valid only for heights of 10–20 cm along the bole. The surface heat flux will decrease with height and the resulting depth of necrosis will decrease accordingly.

The equations in the Results section are based on the heat-flux measurements from the Schmidt–Boelter sensors at the bark surface. Note that these values reflect the heat flux at the sensor surface and not necessarily the flux at the bark. The absorptivity of bark is similar to that of the radiant sensor, so the measured radiative flux is a reasonably accurate estimate of the radiative flux at the bole surface. However, the sensor's radiant flux measurements themselves are subject to uncertainty, so the error may be on the order of 10%–25% (Bryant et al. 2003).

The face of the sensor remains much cooler than the surface of the bark when surrounded by a flame (Jones 2003), implying that the convective flux to the sensor is higher than it is to the bole (because the convective flux depends on the difference between flame and surface temperature). Because of surface temperature differences, the constants in the equations involving the integrated heat flux, Q'', should be considered as scale factors rather than true values.

The coefficient for initial bark moisture was not significantly different from zero ($p > 0.05$, n = 30) in a multivariable linear regression of depth of necrosis versus Q'' and moisture (not shown). Heat outflux by moisture loss was probably directly proportional to incident flux. Therefore, necrotic depth

Fig. 6. A nomogram application of eq. 13. A surface fire with an intensity, I, of 150 kW/m and 20-s residence time results in an estimated depth of necrosis of about 4 mm (upper portion of diagram). This implies that chestnut oaks with less than 2.5 cm DBH will suffer damage below the bark surface, while red maple with diameters less than about 10 cm will be damaged or killed (lower portion of diagram).

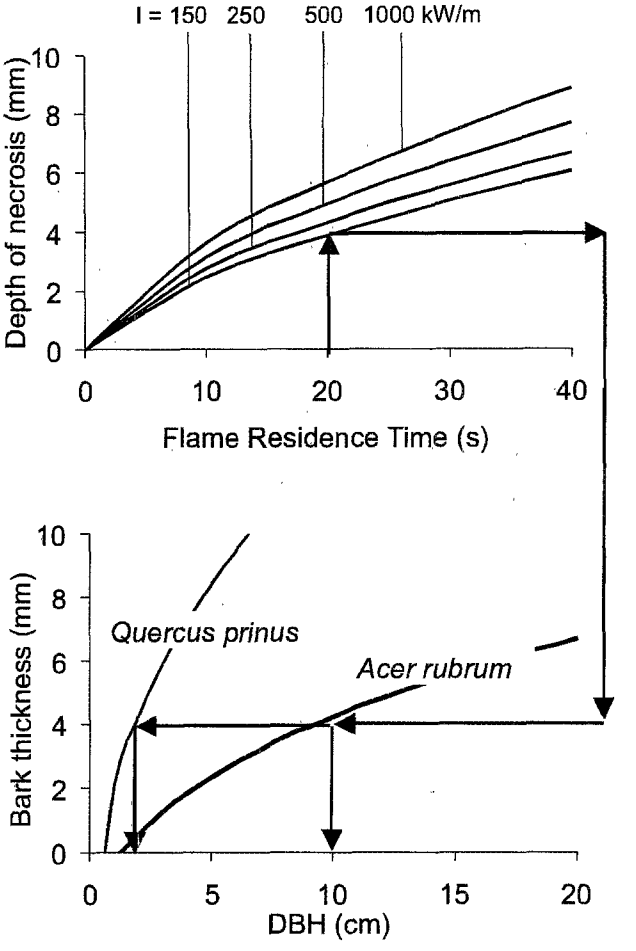

can be calculated without regard to bark moisture, as long as the process of bark drying in fires does not vary extensively among the trees of interest. Another caveat is that heat flux and bark thickness (and, therefore, total moisture content) were correlated in our experiments (Table 1).

Ecological response to stem heating

Because necrotic depth can be estimated from fire intensity and time of flame contact (here taken to be roughly equal to the flame residence time), it may be possible to estimate stem or tree mortality using known relationships between bark thickness and diameter (Fig. 6). Fire intensity and flame residence time correspond to a depth of necrosis that if greater than bark thickness, would be expected to cause vascular cambium necrosis. Bark thickness corresponds to a diameter based on species. In the example, a typical leaf-litter surface fire with an intensity of 150 kW/m and a flame residence time of 20 s corresponds to a depth of ne-

Fig. 7. Red maple and chestnut oak bark-thickness frequency distributions in southern Ohio forests. Profile diagrams were derived from stem diameter at 137 cm (DBH) distributions and relations between bark thickness and DBH. All stems ≥10 cm DBH were measured in plots while stems <10 cm were enumerated in diameter classes (≤4 cm, 4.0–5.9 cm, 6.0–9.9 cm). Kill depths (vertical lines) at a 15 cm height along the bole correspond to increasing intensity, I (kW/m), and flame residence time, t (s), at the bole surface. A height of 15 cm was chosen to correspond to the height of near-maximum heat flux to trees from surface flames.

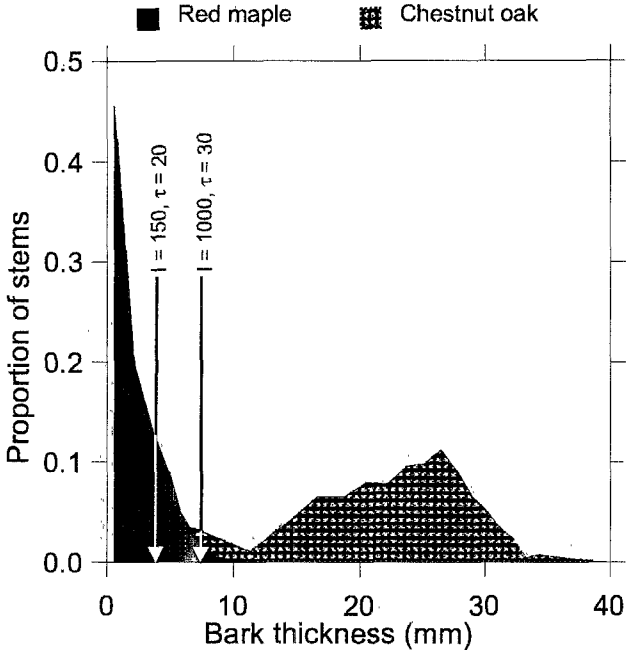

crosis of 4 mm, which would damage or kill (if the heat flux is uniform around the stem) red maple stems with less than 10 cm DBH. A 10-cm maximum DBH for red maple stem kill is, coincidentally, the general rule for prescribed burns in leaf litter in southeastern Ohio. Chestnut oak stems with greater than 2 cm DBH, however, are more likely to survive such a fire according to the nomogram.

Based on our equations, Fig. 7 suggests that red maple populations would be much more negatively affected by surface fires than chestnut oak populations. Historically, Ohio Hills forests burned frequently, a process that largely ceased in the early to middle decades of the 20th century (Sutherland et al. 2003). Since that time, red maples and associated species have increased substantially in abundance, resulting in a general increase in forest stem density. Concomitantly, oaks have regenerated poorly except on the driest sites. Poor oak regeneration is indicated by the bimodal frequency distribution in Fig. 7. A surface fire of very high (for this region) intensity and residence time (~1000 kW/m, $\tau = 30$ s) is also represented in Fig. 7.

Our equations, based on typical surface-fire intensities (50–2000 kW/m), could be used to predict tree mortality before fires are prescribed. Several assumptions must be made, however. (1) We ignore variation in heat flux around stems induced by the interaction between flame flow and cylindrical tree stems (e.g., Gutsell and Johnson 1996). Because uneven heating is an increasing function of tree diameter and the velocity of fluid flow across a stem and because partial vascular cambium necrosis can contribute to tree death, our equations will underestimate stem mortality as diameters increase. (2) Where fuel loading varies spatially, an assumption of constant fuel loading might lead to inadequate predictions of stem mortality. For instance, litter is redistributed among forest patches in Appalachian hardwood forests (Boerner and Kooser 1989). Consequently, trees in different patches would experience a larger range of heating regimes during fires than might be assumed. Ryan and Frandsen (1991) describe concentrations of duff at the base of large ponderosa pines (*Pinus ponderosa* Dougl. ex P. & C. Laws.) and extended basal heating during fires, a situation that would result in substantial bias in stem mortality predictions if not considered. (3) If a stem is invulnerable to surface flames, it still can be killed by canopy heating (Dickinson and Johnson 2001). (4) Stem death does not mean tree death if a stem sprouts from the root collar, a well-known characteristic of oaks and also common in red maples. (5) Wider firelines, especially in high-intensity fires, may result in greater radiative heat transfer to boles, though the data by Wotton et al. (1999) suggest our firelines were of adequate width (and, therefore, the coefficient in eq. 13 is representative). (6) Fire-behavior models would have to give accurate predictions of fire intensity and flame residence time in various weather and slope conditions. Variation in fire behavior across a forest and uncertainty with respect to bark thickness mean that actual predictions should be stated as probabilities rather than as thresholds. (7) Finally, we assume that flame residence time at the bole surface is equal to the flame residence time in the fuel bed, but this may not be true in cases where shifting wind causes either infrequent or extended flame contact with the bole.

We do not know how broadly our results can be applied to other tree species. Although the range of moisture (28%–83%) and diameter (3–17 cm) were reasonably large, only two deciduous species were targeted in these experiments. Species with different bark moistures or thermophysical properties might respond differently to the range of fuel consumption and heat flux generated by our experimental flames.

Conclusion

The strong correlation between the time-integrated heat flux and depth of necrosis indicates that time-integrated heat flux itself is a good estimator of potential depth of necrosis and, if heat flux is roughly uniform around the bole, of stem death in the species studied. A combination of fire intensity and flame residence time at the stem provides the best correlation between fire behavior and tissue necrosis. If the depth of necrosis is greater than bark thickness by a small amount, it is likely that the vascular cambium will be damaged or completely killed. Given known relationships between tree diameter and bark thickness (Fig. 6), and a better understanding of heat transfer to trees during fires, it may be possible to use the relationship in eq. 13 to predict stem and tree mortality in fires of known intensities and residence times over areas large enough that local effects, such as burning slash or shrubs, may be averaged out. An ability to predict

stem and tree mortality would be especially useful for planning prescribed burns.

Acknowledgements

We thank David Hosack, Kristy Tucker, Bill Borovicka, Jim Stockwell, and Brad Tucker of the Vinton Furnace Experimental Forest (VFEF) for assistance with the experimental burns. The VFEF is managed jointly by MeadWestvaco and the Northeastern Research Station. Joan Jolliff helped develop the tissue staining technique. Early discussions with Jim Reardon on tissue necrosis detection were helpful. Dan Jimenez and Bret Butler developed the tree-instrumentation methods and assisted in their implementation. Josh Jones and Brent Webb provided useful discussions on flames and stem heating. Deborah Kennard and James Lenihan provided helpful comments on the manuscript. Dan Yaussy, Matthew Albrecht, and Brian McCarthy provided unpublished sapling and tree data from the Ohio Hills Fire and Fire Surrogate Study. Funding for this project was provided by a grant from the National Fire Plan.

References

Anderson, H.E., and Rothermel, R.C. 1965. Influence of moisture and wind upon the characteristics of free-burning fires. *In* Proceedings of the 10th Symposium (International) on Combustion, Cambridge, UK, 17–21 August 1964. The Combustion Institute, Pittsburgh, Penn. pp. 1009–1019.

Boerner, R.E.J., and Kooser, J.G. 1989. Leaf litter redistribution among forest patches in an Allegheny Plateau watershed. Landsc. Ecol. **2**: 81–92.

Bryant, R., Womeldorf, C., Johnsson, E., and Ohlemiller, T. 2003. Radiative heat flux measurement uncertainty. Fire Mater. **27**: 209–222.

Caldwell, C.R. 1993. Estimation and analysis of cucumber (*Cucumis sativus* L.) leaf cellular heat sensitivity. Plant Physiol. **101**: 939–945.

Costa, J.J., Oliveira, L.A., Viegas, D.X., and Neto, L.P. 1991. On the temperature distribution inside a tree under fire conditions. Int. J. Wildl. Fire, **1**: 87–96.

Dickinson, M.B. 2002. Heat transfer and vascular cambium necrosis in the boles of trees during surface fires. *In* Forest fire research and wildland fire safety. *Edited by* X. Viegas. [CD-ROM]. Millpress, Rotterdam, Netherlands.

Dickinson, M.B., and Johnson, E.A. 2001. Fire effects on trees. *In* Forest fires: behavior and ecological effects. *Edited by* E.A. Johnson and K. Miyanishi. Academic Press, New York. pp. 477–525.

Dickinson, M.B., and Johnson, E.A. 2004. Temperature-dependent rate models of vascular cambium necrosis. Can. J. For. Res. **34**: 546–559.

Dickinson, M.B., Jolliff, J., and Bova, A.S. 2004. Vascular cambium necrosis in forest fires: using hyperbolic temperature regimes to estimate parameters of a tissue-response model. Aust. J. Bot. **52**(6): 757–763.

Fons, W.L. 1946. Analysis of fire spread in light forest fuels. J. Agric. Res. **72**: 93–121.

Gutsell, S.L., and Johnson, E.A. 1996. How fire scars are formed: coupling a disturbance process to its ecological effect. Can. J. For. Res. **26**: 166–174.

Hare, R.C. 1961. Heat effects on living plants. USDA For. Serv. South. For. Exp. Stn. Occas. Pap. 183.

Incropera, F.P., and DeWitt, D.P. 2002. Introduction to heat transfer. John Wiley & Sons, Inc., New York.

Johnson, E.A. 1992. Fire and vegetation dynamics. Cambridge University Press, Cambridge, UK.

Johnson, F.H., Eyring, H., and Stover, B.J. 1974. The theory of rate processes in biology and medicine. John Wiley & Sons, Inc., New York.

Jones, J.L. 2003. Development of a model for predicting stem mortality under fire conditions. M.Sc. thesis, Brigham Young University, Provo, UT.

Jones, J.L., Webb, B.W., Jimenez, D., Reardon, J., and Butler, B. 2004. Development of an advanced one-dimensional stem heating model for application in surface fires. Can. J. For. Res. **34**: 20–30.

Kayll, A.J. 1963. Heat tolerance of Scots pine seedling cambium using tetrazolium chloride to test viability. Can. Dep. For. For. Res. Branch Publ. 1006.

Levitt, J. 1980. Responses of plants to environmental stresses. Vol. I: chilling, freezing, and high temperature stresses, 2nd ed. Academic Press, New York.

Lorenz, R. 1939. High temperature tolerance of forest trees. University of Minnesota, Agricultural Experiment Station, St. Paul, Minn. Tech. Bull. 141.

Mardini, J.A., Lavine, A.S., and Dhir, V.K. 1996. Heat and mass transfer in wooden dowels during simulated fire: an experimental and analytical study. Int. J. Heat Mass Transfer, **39**: 2641–2651.

Martin, R.E. 1961. Thermal and other properties of bark and their relation to fire injury of tree stems. Ph.D. dissertation, University of Michigan, Ann Arbor, Mich.

Martin, R.E., Cushwa, C.T., and Miller, R.L. 1969. Fire as a physical factor in wildland management. Proc. Tall Timbers Fire Ecol. Conf. **9**: 271–288.

Mercer, G.N., and Weber, R.O. 2001. Fire plumes. *In* Forest fires: behavior and ecological effects. *Edited by* E.A. Johnson and K. Miyanishi. Academic Press, New York. pp. 225–255.

Mercer, G.N., Gill, A.M., and Weber, R.O. 1994. A time-dependent model of fire impact on seed survival in woody fruits. Aust. J. Bot. **42**: 71–81.

Nelson, R.M., and Adkins, C.W. 1986. Flame characteristics of wind-driven surface fires. Can. J. For. Res. **16**: 1293–1300.

Nelson, R.M., and Adkins, C.W. 1988. A dimensionless correlation for the spread of wind-driven fires. Can. J. For. Res. **18**: 391–397.

Parker J. 1953. Some applications and limitations of tetrazolium chloride. Science (Washington, D.C.), **118**: 77–79.

Peterson, D.L., and Ryan, K.C. 1986. Modeling postfire conifer mortality for long-range planning. Environ. Manage. **10**: 797–808.

Pinard, M.A., and Huffman, J. 1997. Fire resistance and bark properties of trees in a seasonally dry forest in eastern Bolivia. J. Trop. Ecol. **13**: 727–740.

Potter, B.E., and Andresen, J.A. 2002. A finite-difference model of temperatures and heat flow within a tree stem. Can. J. For. Res. **32**: 548–555.

Rego, F., and Rigolot, E. 1990. Heat transfer through bark — a simple predictive model. *In* Fire in ecosystem dynamics. *Edited by* J.G. Goldammer and M.J. Perkins. SPB Academic Publishing, The Hague, Netherlands. pp. 157–161.

Ryan, K.C., and Frandsen, W.H. 1991. Basal injury from smoldering fires in mature *Pinus ponderosa* Laws. Int. J. Wildl. Fire, **1**: 107–118.

Systat Software, Inc. 1998. SYSTAT version 9 [computer program]. Point Richmond, Calif.

Sutherland, E.K., Hutchinson, T.F., and Yaussy, D.A. 2003. Introduction, study and description, and experimental design. *In* Characteristics of mixed-oak forest ecosystems in southern Ohio prior to the reintroduction of fire. *Edited by* E.K. Sutherland and T.F. Hutchinson. USDA For. Serv. Gen. Tech. Rep. NE-299. pp. 1–16.

Towill, L.E., and Mazur, P. 1975. Studies on the reduction of 2,3,5-triphenyltetrazolium chloride as a viability assay for plant tissue cultures. Can. J. Bot. **53**: 1097–1102.

Uhl, C., and Kauffman, J.B. 1990. Deforestation fire susceptibility, and potential tree responses to fire in the eastern Amazon. Ecology, **71**(2): 437–449.

Van Wagner, C.E. 1973. Height of crown scorch in forest fuels. Can. J. For. Res. **3**: 373–378.

Van Wagner, C.E. 1977. Conditions for the start and spread of a crown fire. Can. J. For. Res. **7**: 23–34.

Wotton, B.M., McAlpine, R.S., and Hobbs, M.W. 1999. The effect of fire front width on surface fire behaviour. Int. J. Wildland Fire. **9**(4): 247–253.

Yuan, L.M., and Cox, G. 1996. An experimental study of some line fires. Fire Safety J. **27**: 123–139.